# **RSC Advances**



## **PAPER**

View Article Online
View Journal | View Issue



Cite this: RSC Adv., 2022, 12, 17257

# The effect of heteroatom doping on the active metal site of CoS<sub>2</sub> for hydrogen evolution reaction

Jianjian Shi, pa Tao Chen\* and Xiaoli Sun\*bc

The exploration of cost-effective hydrogen evolution reaction (HER) electrocatalysts through water splitting is important for developing clean energy technology and devices. The application of  $CoS_2$  in HER has been drawing more and more attention due to its low cost and relatively satisfactory HER catalytic performance. And  $CoS_2$  was found to exhibit excellent HER catalytic performance after appropriate doping according to other experimental investigations. However, the theoretical simulation and the intrinsic catalytic mechanism of  $CoS_2$  remains insufficiently investigated. Therefore, in this study, density functional theory is used to investigate the HER catalytic activity of  $CoS_2$  doped with a heteroatom. The results show that Pt-, N- and O-doped  $CoS_2$  demonstrates smaller Gibbs free energies close to that of Pt, compared with the original  $CoS_2$  and  $CoS_2$  doped with other atoms. Furthermore, HER catalytic performance of  $CoS_2$  can be improved by tuning d-band centers of H adsorption sites. This study provides an effective method to achieve modified  $CoS_2$  for high-performance HER and to investigate other transition metal sulfides as HER electrode.

Received 23rd March 2022 Accepted 1st June 2022

DOI: 10.1039/d2ra01865a

rsc li/rsc-advances

#### 1 Introduction

The high combustion heat value, clean combustion products, and abundant resources make hydrogen  $(H_2)$  a distinguished energy storage material. Producing hydrogen from the electrochemical decomposition of water  $(H_2O)$ , the commonly believed future energy carrier,  $^{1,2}$  through hydrogen evolution reaction (HER) has been proved to be a clean and renewable method. However, the hydrogen production catalyst precious metal platinum (Pt), the most efficient electrocatalyst for HER owing to its high stability, low overpotential (about 0.08 V), as well low Tafel slope, has not been applied on large scales due to its high cost and scarcity. Hence, it is quite necessary to find a new high-performance HER catalyst.

In recent decades, transition metal sulfides (TMSs), such as  $MoS_2$ ,  $^{4-10}$  VS $_2$ ,  $^{11-15}$  CoS $_2$ ,  $^{2,16-20}$  NiS $_2$  (ref. 2, 7, 15, 21 and 22) have been attracting attention from researchers and industry practitioners. Though the effects of the aforesaid compounds as hydrogen production catalysts had been considered in some previous studies, the more recent ones show that some of them such as HER electrode material can exhibit outstanding electrocatalytic performance that is close to that of precious metals (such as Pt). To further optimize the performance of the TMSs, some other studies suggest the incorporating of a third

As a representative of pyrite-type transition metal sulfides,  $CoS_2$  is a low-cost catalytic material with excellent HER performance. Unfortunately, when doping  $CoS_2$  with a third heteroatom, no good descriptor can be found to describe the relationship between the structure and activity of the doped  $CoS_2$ , and the inherent mechanism remains insufficiently explored.

It is noteworthy that Hoffmann *et al.* found that the center of the d-band formed by the TM turned out to be a good descriptor to predict the adsorption and reactivity of transition metal catalysts. Furthermore, an analogous model of d-band based on surface resonance states has also been developed in the transition metal carbides (TMCs), metal nitrides (MNs), and layered TMSs. This can significantly contribute to the analysis of structure–activity relationships in TMCs/TMSs, which can further help improve the design and high-throughput screening of catalysts. Many studies have also found that doping can change the energy band structure near the Fermi energy, so as to change the properties of materials. 10,28,29 Therefore, we take interest in investigating the possibility to doped CoS<sub>2</sub> for high-performance HER by tuning the d-band centers.

In this work, we study the effect of a heteroatom doping on HER electrochemical properties for  $CoS_2$  electrode material based on density functional theory and explore the structure–activity relationships. Herein, the models of the pristine  $CoS_2$  and doped  $CoS_2$  were built, the stability, the catalytic activity, and the d-band centers of the active metal sites of  $CoS_2$  doped with a heteroatom (Mn, Fe, Ni, Cu, Mo, Pt, Ru, C, N, O, P) are

heteroatom in a binary compound, which can improve the electrocatalytic activity of the catalyst.<sup>23</sup>

<sup>&</sup>quot;School of Electronic Engineering, Chengdu Technological University, Chengdu 611730, PR China. E-mail: sjjian@cdtu.edu.cn; 570560423@qq.com

<sup>&</sup>lt;sup>b</sup>Department of Energy and Power Engineering, Tsinghua University, Beijing, 100084, P. R. China. E-mail: sunxiaolideyuye@163.com

Beijing Graphene Institute, Beijing 100095, P. R. China

**RSC Advances** 

studied based on density functional theory (DFT). Our firstprinciples calculations exhibit that the structures of all doped CoS2 except C-doped CoS2 are stable, the catalytic behavior of CoS<sub>2</sub> can be effectively enhanced after Pt, N, and O doping, and the HER catalysis of CoS<sub>2</sub> can be changed by tailoring the dband centers of active metal sites. Our studies are of great benefit to uncovering the intrinsic modulation mechanism of CoS<sub>2</sub> for HER catalysis.

## Computational methods

All density functional theory (DFT) simulations were employed using the Generalized Gradient Approximation-Perdew Burke Ernzerhof (GGA-PBE) was used for the exchange-correlation term in the Spanish Initiative for Electronic Simulations with Thousands of Atoms (SIESTA).30,31 The geometric optimization was employed using a conjugate gradient method until the maximum force was less than 0.02 eV  $\mathring{A}^{-1}$ . An energy cut-off for all simulations was set to be 150 Ry.

#### 2.1 Bulk CoS<sub>2</sub>

The k-point mesh is set as  $\Gamma$ -centered 7 × 7 × 7 to relax the CoS<sub>2</sub> unit cell with a space group of  $Pa\bar{3}$ . The calculated  $CoS_2$  unit cell parameter is 5.544 Å, which is highly consistent with the experimental value (5.538 Å).<sup>23,32</sup> The optimized bulk structure is shown in Fig. 1, where the big and small balls represent Co and S atoms, respectively.

#### 2.2 CoS<sub>2</sub>(001) surface

The (001) surface of CoS<sub>2</sub> is selected as the optimization model owing to its stability,32 which is built as a 2 × 2 repeating surface unit cells consisting of four S-Co-S atomic layers and 8 CoS<sub>2</sub> units. Cation-doped CoS<sub>2</sub> is acquired by replacing one Co atom with one metal atom, and anion-doped CoS2 is acquired by replacing one S atom with one nonmetal atom. A vacuum layer with a thickness of 15 Å is introduced to reduce interaction between periodic images.33 The CoS2(001) crystalline structure is represented in Fig. 2.

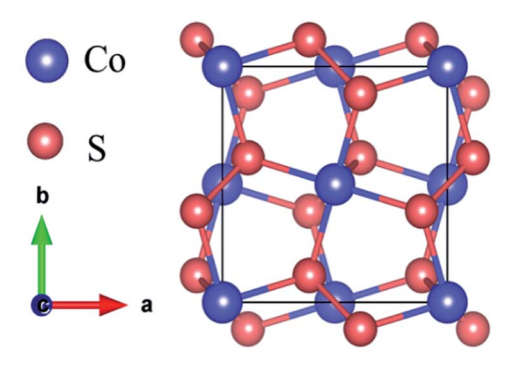
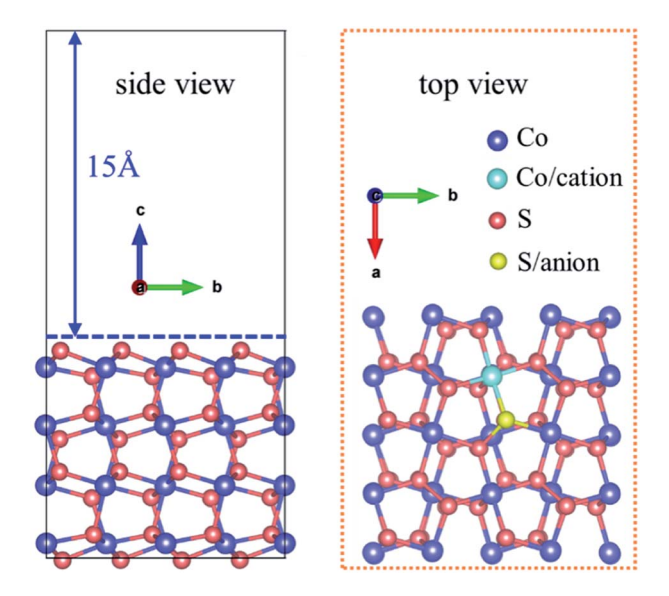


Fig. 1 The optimized structure of the bulk CoS<sub>2</sub>.



The crystallographic structure of CoS<sub>2</sub>(001) surface

#### **Binding energy**

The binding energies  $(E_b)$  were first calculated to measure the stability of  $CoS_2$  after doping,  $E_b$  is the difference between the cohesive energy  $(E_{coh})$  of cubic  $CoS_2$  and the embedding energy of the dopants ( $E_{emb}$ ) on the CoS<sub>2</sub> surface.<sup>34</sup>

$$E_{\rm coh} = E_{\rm bulk} - E_{\rm iso} \tag{1}$$

$$E_{\rm emb} = E_{\rm dopant+subs} - E_{\rm subs} - E_{\rm iso} \tag{2}$$

$$E_{\rm b} = E_{\rm coh} - E_{\rm emb} \tag{3}$$

where  $E_{\text{bulk}}$  is the total energy of an atom in the bulk,  $E_{\text{iso}}$  is the total energy of an isolated atom,  $E_{dopants+subs}$  is the total energy of doped  $CoS_2$ , and  $E_{subs}$  is the total energy of  $CoS_2$  with one vacancy.

#### 2.4 Gibbs free energy of H adsorption

Nørskov et al.3 showed that with the absolute Gibbs free energy of hydrogen adsorption ( $\Delta G_{H^*}$ ) approximating zero, the binding between HER intermediates and the electrode surface was neither too strong nor too weak, demonstrating a high catalytic performance of HER. Hence, the  $(\Delta G_{H^*})$  as a significant factor of measuring the HER catalytic activity is quite essential to is calculated using reliable DFT simulations.35 In our work, the HER catalytic properties in acidic media were investigated. While considering the HER reaction process in acid, the Volmer reaction3 was selected under our calculations, because most reactions occur in protic solution or involve proton as the reactant:  $^{36}$  H<sup>+</sup>(sol) + e<sup>-</sup>  $\rightarrow$  H\*, where H\* refers to H adsorbed on the active site, and many studies analyze the electrochemical catalytic properties of HER based on the Volmer reaction.<sup>3</sup> The Gibbs free energy of hydrogen adsorption ( $(\Delta G_{H^*})$ ) as a significant factor of measuring the HER catalytic activity is calculated

Paper RSC Advances

Table 1 Binding energies of doped  $CoS_2$  ( $E_b$ , eV)

Cation	Model E <sub>b</sub> /eV					Mo −1.78		Ru -1.97
Anion	Model E <sub>b</sub> /eV		C 1.96	N -	-1 <b>.</b> 67	O -2.2	27	P -1.52

based on the Volmer reaction using the DFT method. Its definition is as follows<sup>35</sup>

$$\Delta G_{H^*} = \Delta E_H + \Delta E_{ZPE} - T\Delta S \tag{4}$$

where  $\Delta E_{\rm ZPE}$  is the difference in zero-point energy between the adsorption state of H and gas phase, while  $\Delta S$  is the difference in entropy between the adsorption state of H and gas phase.<sup>3</sup>  $\Delta E_{\rm H}$  is the hydrogen adsorption energy. Given that the vibrational entropy of H\* in the adsorbed state is small, the entropy of adsorption of  $-1/2{\rm H}_2$  is simplified as  $\Delta S_{\rm H} \approx -1/2S_{{\rm H}_2}{}^0$ , where  $S_{{\rm H}_2}{}^0$  is the entropy of H<sub>2</sub> in the gas phase at standard conditions. Therefore, the overall corrections of  $\Delta G_{{\rm H}^*}$  are<sup>3</sup>

$$\Delta G_{H^*} = \Delta E_H + 0.24 \text{ eV} \tag{5}$$

The hydrogen adsorption energy ( $\Delta E_{\rm H}$ ) on the electrode surfaces is defined as

$$\Delta E_{\rm H} = E_{\rm subs+H^*} - E_{\rm subs} - \frac{1}{2} E_{\rm H_2} \tag{6}$$

where  $E_{\text{subs}+\text{H}^*}$  is the total energy of doped  $\text{CoS}_2(001)$  with H\* adsorption,  $E_{\text{subs}}$  is the total energy of doped  $\text{CoS}_2(001)$  without

 $H^*$  adsorption, and  $E_{H_2}$  is the total energy for one hydrogen molecule in the gas phase.

#### 2.5 d-band centers

To further explore the possibility of enhancing electrochemical performance of CoS<sub>2</sub> *via* doping, we calculated the d-band center of the metal at active site.

The d-band center  $\varepsilon_d$  is defined as

$$\varepsilon_{\rm d} = \frac{\int_{-\infty}^{\infty} \rho(\varepsilon) \varepsilon d\varepsilon}{\int_{-\infty}^{\infty} \rho(\varepsilon) d\varepsilon} \tag{7}$$

where  $\rho$  are the densities of states and  $\varepsilon$  are the energies.

## 3 Results and discussion

Some materials demonstrate good computational performance but are difficult to synthesize due to their aggregation- or clustering-related instability, which limits their application in experiments or in practice.37 So, it is important to first investigate the stability of CoS<sub>2</sub> in order to explore the possibility of its synthesis. We use the binding energy  $(E_b)$  descriptor to measure the stability of doped  $CoS_2$ , if,  $E_b < 0$ , the atoms shows more tendency of being incorporated into the CoS2(001) surface rather than clustering or aggregation, and then we regard that the material satisfies the stability criterion.34 The calculated binding energies are listed in Table 1. From Table 1 we can see,  $E_{\rm b}$  of all cation and anion doped  $CoS_2$  except for C-doped  $CoS_2$ are less than zero, which demonstrates that it is energetically possible for one cation dopant to replace one Co atom in the CoS<sub>2</sub>(001) surface and for one anion dopant to replace one S atom in the CoS<sub>2</sub>(001) surface. However, the binding energy is

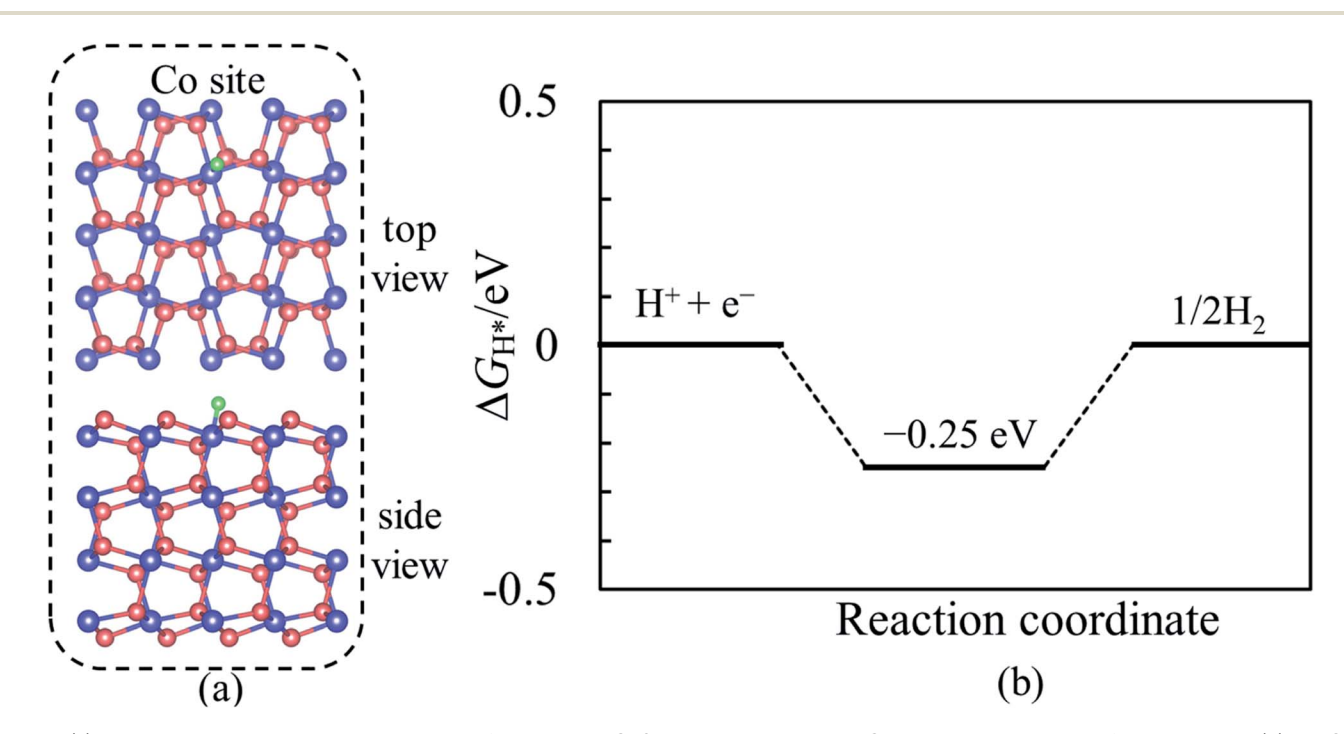


Fig. 3 (a) Represents the H adsorption structure of the pristine  $CoS_2$ , where H adsorbs at Co site. The green ball refers to H atom. (b) is  $\Delta G_{H^*}$  diagram of the pristine  $CoS_2$ .

1.96 eV when one S atom in the  $CoS_2(001)$  surface is substituted by one C atom, which is much higher than zero, indicating that when one C is incorporated into the  $CoS_2(001)$ , it tends to take the form of cluster or aggregation, which causes an unstable C-doped  $CoS_2(001)$  structure. Therefore, C will not be considered as a heteroatom to form a HER catalyst.

After identifying the stability for a cation/anion heteroatom incorporated into the  $CoS_2(001)$  surface, the state of the adsorbed H was discussed according to H adsorption energy. The negative value means that H is easy to bind to the  $CoS_2(001)$ . The value of adsorption energy for 11 doped- $CoS_2$  are from -1.43 eV to -2.46 eV, which indicates that it is feasible to H bind to the surface of  $CoS_2(001)$ . Moreover, the catalytic performance for HER of the  $CoS_2(001)$  with and without cation/anion heteroatom doping was investigated. To determine whether  $CoS_2$  is an outstanding HER catalyst, the Gibbs free energies ( $\Delta G_{H^*}$ ) for hydrogen adsorption at active metal sites were calculated based on the DFT method. Fig. 3(a) is the relaxed crystallographic structure of H adsorption at the Co site for the pure  $CoS_2(001)$ , in which the green ball refers to H atom.

The Co-H bond length is 1.50 Å. The calculated  $|\Delta G_{H^*}|$  of the pure CoS<sub>2</sub>(001) is 0.25 eV, as shown in Fig. 3(b), which is larger than that of the precious metal Pt (0.08 eV).3 In order to further probe the effect of heteroatom atoms on electrochemical HER catalytic performance for CoS<sub>2</sub>(001) as electrode material, the  $\Delta G_{H^*}$  of cation- (Mn, Fe, Ni, Cu, Mo, Pt and Ru) and anion- (N, O and P) doped CoS<sub>2</sub> are calculated using the DFT method. Fig. 4(a) and (c) show the calculated  $\Delta G_{H^*}$  of H adsorption at the active metal sites for cation- and anion-doped CoS2(001), respectively. In Fig. 4(a) and (c),  $\Delta G_{H^*}$  of Ni-doped CoS<sub>2</sub>(001) is -0.12 eV, that of Pt-doped  $CoS_2(001)$  is 0.03 eV, that of N-doped  $CoS_2(001)$  is 0.07 eV, and that of O-doped  $CoS_2(001)$  is -0.01 eV. Compared with that (0.25 eV) of the pure CoS<sub>2</sub> electrode, the  $|\Delta G_{H^*}|$  of Ni-, Pt-, N-, and O-doped  $CoS_2(001)$  electrode are much smaller when H is adsorbed at metal sites. It is noteworthy that  $|\Delta G_{H^*}|$  of Pt-, N-, and O-doped  $CoS_2(001)$  is smaller than that of Pt (0.08 eV), revealing their potential excellent electrochemical HER catalytic performance. And  $|\Delta G_{H^*}|$  of O-doped CoS<sub>2</sub>(001) is closest to zero, which suggests that O-doped CoS2 show the best HER catalytic activity among these doped CoS<sub>2</sub> material.

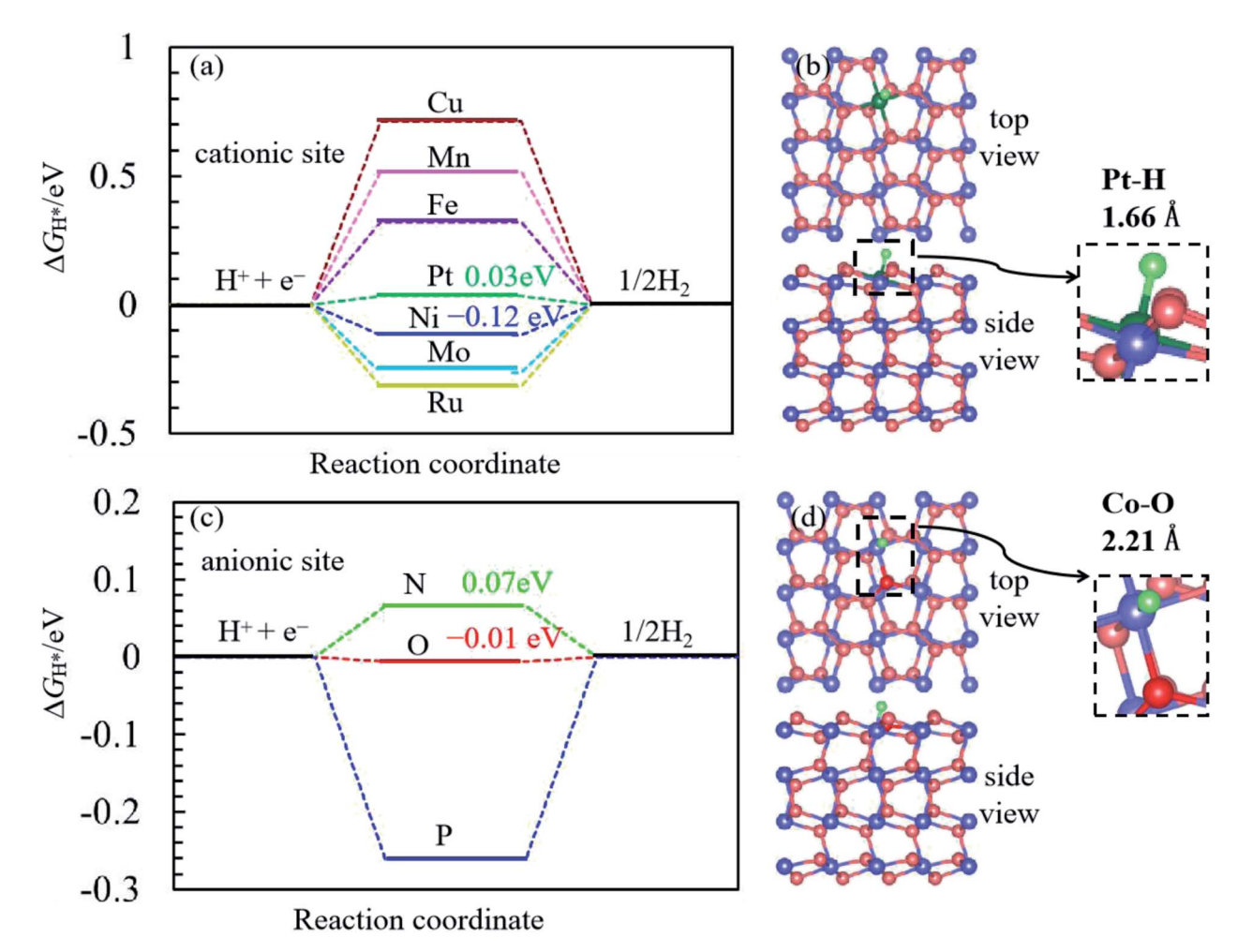


Fig. 4 (a) and (b) are  $\Delta G_{H^*}$  diagram and the structure of Pt-doped CoS<sub>2</sub>(001) with H adsorption at Pt site, respectively. (c) and (d) are  $\Delta G_{H^*}$  diagram and the structure of O-doped CoS<sub>2</sub>(001) with H adsorption at Co site, respectively. The blue, dark green, red balls and light green ball are Co, S, Pt, O and H atoms, respectively. Pt-H bond length is 1.66 Å and Co-O bond length is 2.21 Å.

Fig. 4(b) and (d) show the optimized structures of the Pt-doped CoS<sub>2</sub>(001) with H adsorption at Pt site, Pt-H bond length is 1.66 Å, and that of the O-doped CoS<sub>2</sub>(001) with H adsorption at Co site, Co-H bond length is 1.51 Å, respectively. To further explore why the electrochemical HER performance of CoS<sub>2</sub> at active metal sites via doping can be enhanced, the d-band centers of the active metal sites were calculated using the DFT method. We plotted in Fig. 5 the density of states for active metal sites used to H adsorption and marked the d-band center at active metal site with a dashed line. The d-band center of Co active site for the pristine  $CoS_2$  is -2.06 eV and it is closest to the Fermi level. The d-band center of Cu active site for Cu-doped CoS2 is -6.01 eV and it is farthest to the Fermi level. Meanwhile,  $\Delta G_{H^*}$ for Cu-doped CoS<sub>2</sub> is 0.71 eV. To further probe the relationship between the d-band center of active metal site used to H adsorption and the Gibbs free energy of H adsorption on the active metal sites, a more detailed analysis diagram is plotted in Fig. 6. We can see from Fig. 6 that  $\Delta G_{H^*}$  increases as the d-band

centers of metal active sites decrease, which clearly illustrates that the binding between H adsorption atom and metal atom at the active site is weakened as the d band center is far away from the Fermi level. Our results just described are in line with investigations in the  $\Delta G_{\mathrm{H}^*}$  and d-band centers based on other materials. This study reveals an intrinsic mechanism that d-band center of active metal site moves downwards after doping, leading to the weakening of hydrogen adsorption, which facilitates the desorption of H from the surface of  $\mathrm{CoS}_2$  as HER electrode material.

Based on our DFT calculations, we can find that Ni-, Pt-, O-, and N-doping can intrinsically promote the electrochemical HER catalytic performance of  $CoS_2$  and a line in  $\Delta G_{H^*}$  and d-band centers of H adsorption sites is achieved. The Pt-, O-, and N-doped  $CoS_2$  show overpotentials of 0.03 V, 0.01 V, and 0.07 V, respectively, which are very close to values when using Pt, which is believed to be the best catalyst for the HER because

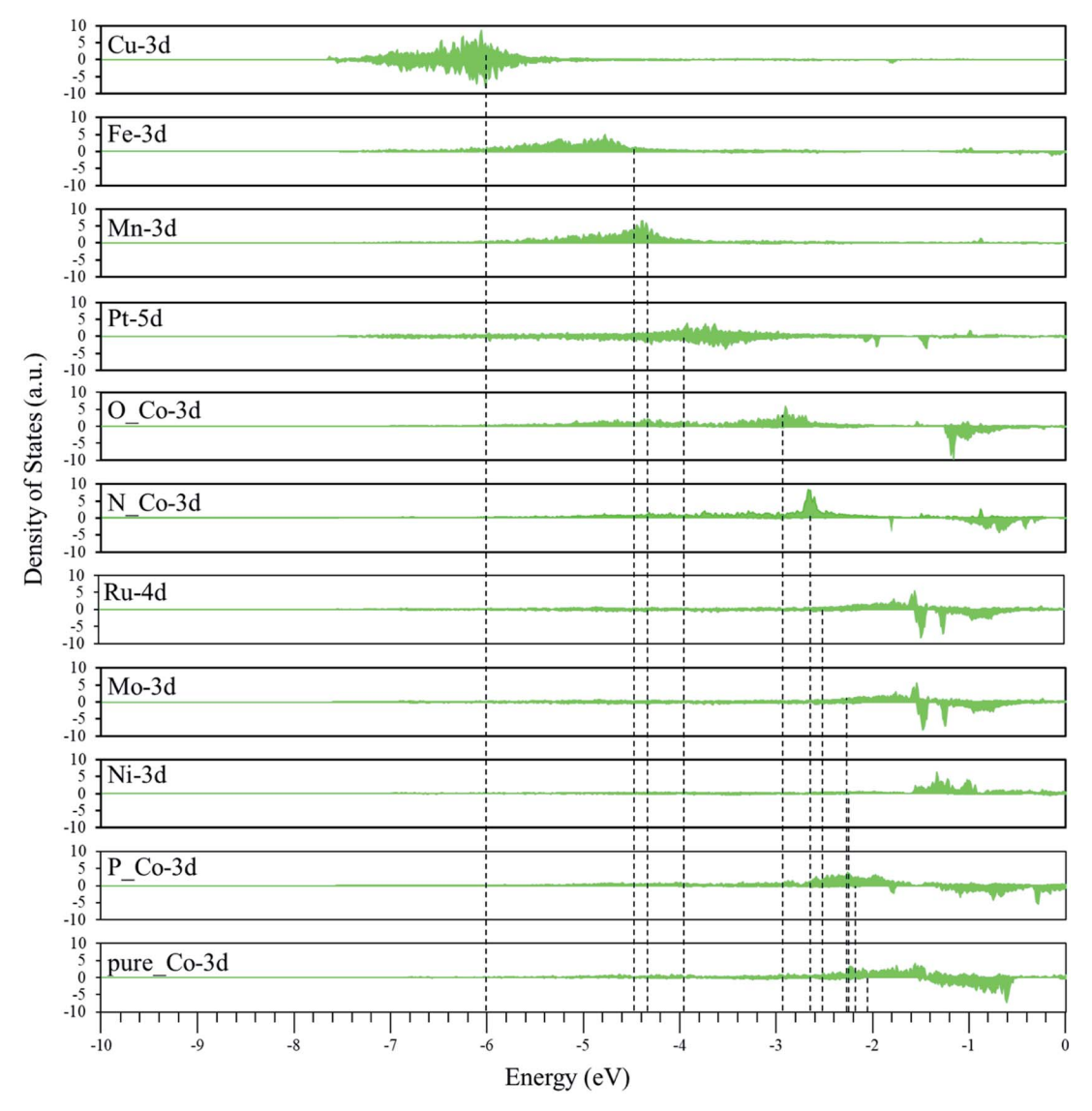


Fig. 5 The density of states at active metal sites. The dashed line marked the d-band center. The Fermi energy is set to zero.

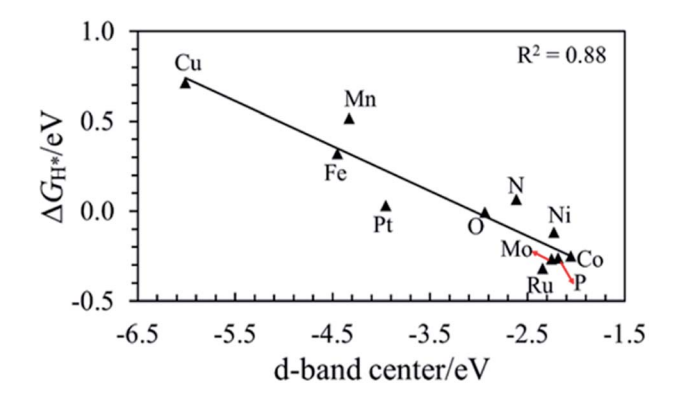


Fig. 6 The linear relationship between  $\Delta G_{H^*}$  and d-band centers of H adsorption sites.

of its small overpotential (about 0.08 V).<sup>3</sup> Therefore, the CoS<sub>2</sub>, after doping by Pt, O, and N becomes a promising catalyst.

#### 4 Conclusions

In summary, we studied HER catalytic activities of cation/anion-doped  ${\rm CoS_2}$  as HER catalyst based on the DFT method. Our results reveal that the Pt-, N- and O-doped  ${\rm CoS_2}$  possesses an outstanding HER catalytic activity comparable to Pt. And a negative linear relationship was identified between  $\Delta G_{\rm H^*}$  and d-band centers of active metal sites. This exhibits that d-band center of active metal site moves downwards after cation/anion doping, leading to the weakening of hydrogen adsorption and facilitating the H desorption from the surface of  ${\rm CoS_2}$ . Therefore, the intrinsic HER catalytic performance of  ${\rm CoS_2}$  can be improved by tailoring the d-band center of the active metal site. Based on this study, we can further explore the relationship between the structure and activity of  ${\rm CoS_2}$ , which may shed light on the exploration of the potential use of other TMSs as HER electrode materials.

#### Conflicts of interest

There are no conflicts to declare.

## Acknowledgements

This work is supported by the Fund Project of Chengdu Technological University under Grant No. 2020RC004.

#### References

- 1 Y. Tachibana, L. Vayssieres and J. R. Durrant, *Nat. Photonics*, 2012, 6, 511–518.
- 2 B. Qiu, Y. Zhang, X. Guo, Y. Ma, M. Du, J. Fan, Y. Zhu, Z. Zeng and Y. Chai, J. Mater. Chem. A, 2022, 10, 719–725.
- 3 J. K. Nørskov, T. Bligaard, A. Logadottir, J. R. Kitchin, J. G. Chen, S. Pandelov and U. Stimming, *ChemInform*, 2005, **152**, L5.
- 4 D. Saha, V. Patel, P. R. Selvaganapathy and P. Kruse, *Nanoscale Adv.*, 2022, 4, 125–137.

- 5 B. Hinnemann, P. G. Moses, J. Bonde, K. P. Jørgensen, J. H. Nielsen, S. Horch, I. Chorkendorff and J. K. Nørskov, J. Am. Chem. Soc., 2005, 127, 5308–5309.
- 6 R. Li, J. Liang, T. Li, L. Yue, Q. Liu, Y. Luo, M. S. Hamdy, Y. Sun and X. Sun, *Chem. Commun.*, 2022, 15, 633–644.
- 7 J. Tian, X. Xing, Y. Sun, X. Zhang, Z. Li, M. Yang and G. Zhang, Chem. Commun., 2022, 58, 557–560.
- 8 S. Mansingh, K. K. Das and K. Parida, Sustainable Energy Fuels, 2021, 5, 1952–1987.
- 9 H. Wang, X. Xiao, S. Liu, C.-L. Chiang, X. Kuai, C.-K. Peng, Y.-C. Lin, X. Meng, J. Zhao, J. Choi, Y.-G. Lin, J.-M. Lee and L. Gao, J. Am. Chem. Soc., 2019, 141, 18578–18584.
- 10 J. Lee, J. Heo, H. Y. Lim, J. Seo, Y. Kim, J. Kim, U. Kim, Y. Choi, S. H. Kim, Y. J. Yoon, T. J. Shin, J. Kang, S. K. Kwak, J. Y. Kim and H. Park, ACS Nano, 2020, 14, 17114–17124.
- 11 Y. Qu, H. Pan, C. Tat Kwok and Z. Wang, Phys. Chem. Chem. Phys., 2015, 17, 24820-24825.
- 12 Y. Lin, M. Yu, X. Li, W. Gao, L. Wang, X. Zhao, M. Zhou, X. Yao, M. He and X. Zhang, J. Mater. Chem. C, 2021, 9, 15877–15885.
- 13 J. Xu, Y. Zhu, B. Yu, C. Fang and J. Zhang, *Inorg. Chem. Front.*, 2019, **6**, 3510–3517.
- 14 Z. Wang, K. Yu, R. Huang and Z. Zhu, *CrystEngComm*, 2021, 23, 5097–5105.
- 15 N. Ran, B. Sun, W. Qiu, E. Song, T. Chen and J. Liu, *J. Phys. Chem. Lett.*, 2021, **12**, 2102–2111.
- 16 G. Chen, H. Li, Y. Zhou, C. Cai, K. Liu, J. Hu, H. Li, J. Fu and M. Liu, *Nanoscale*, 2021, 13, 13604–13609.
- 17 Y. Dong, H. Sun and G. Liu, Sustainable Energy Fuels, 2021, 5, 4115–4125.
- 18 Z. Shi, X. Qi, Z. Zhang, Y. Song, J. Zhang, C. Guo, W. Xu, K. Liu and Z. Zhu, *Nanoscale*, 2021, **13**, 6890–6901.
- 19 Y. Jiang, S. Gao, J. Liu, G. Xu, Q. Jia, F. Chen and X. Song, *Nanoscale*, 2020, **12**, 11573–11581.
- 20 Y. Zang, B. Yang, A. Li, C. Liao, G. Chen, M. Liu, X. Liu, R. Ma and N. Zhang, ACS Appl. Mater. Interfaces, 2021, 13, 41573– 41583.
- 21 C. n. Karakaya, N. Solati, U. Savacı, E. Keleş, S. Turan, S. Çelebi and S. Kaya, *ACS Catal.*, 2020, **10**, 15114–15122.
- 22 C. Karakaya, N. Solati, U. Savacı, E. Keleş, S. Turan, S. Çelebi and S. Kaya, *ACS Catal.*, 2020, **10**, 15114–15122.
- 23 J. Zhang, Y. Liu, B. Xia, C. Sun, Y. Liu, P. Liu and D. Gao, *Electrochim. Acta*, 2018, **259**, 955–961.
- 24 G. Papoian, J. K. Nørskov and R. Hoffmann, *J. Am. Chem. Soc.*, 2000, **122**, 4129–4144.
- 25 A. Vojvodic, A. Hellman, C. Ruberto and B. I. Lundqvist, *Phys. Rev. Lett.*, 2009, **103**, 146103.
- 26 Z. Chen, Y. Song, J. Cai, X. Zheng, D. Han, Y. Wu, Y. Zang, S. Niu, Y. Liu, J. Zhu, X. Liu and G. Wang, *Angew. Chem.*, *Int. Ed.*, 2018, 57, 5076–5080.
- 27 C. Tsai, K. Chan, J. K. Nørskov and F. Abild-Pedersen, *J. Phys. Chem. Lett.*, 2014, 5, 3884–3889.
- 28 A. Maibam, S. Krishnamurty and M. Ahmad Dar, *Mater. Adv.*, 2022, 3, 592–598.
- 29 A. Maibam, S. K. Das, P. P. Samal and S. Krishnamurty, *RSC Adv.*, 2021, **11**, 13348–13358.

- 30 J. M. Soler, E. Artacho, J. D. Gale, A. García, J. Junquera, P. Ordejón and D. Sánchez-Portal, *J. Phys.: Condens. Matter*, 2002, **14**, 2745–2779.
- 31 J. P. Perdew, K. Burke and M. Ernzerhof, *Phys. Rev. Lett.*, 1996, 77, 3865–3868.
- 32 J. Zhang, Y. Liu, C. Sun, P. Xi, S. Peng, D. Gao and D. Xue, *ACS Energy Lett.*, 2018, 3, 779–786.
- 33 J. Shi, Z. Wang and Y. Q. Fu, *J. Phys. D: Appl. Phys.*, 2016, 49, 505601.
- 34 W. I. Choi, B. C. Wood, E. Schwegler and T. Ogitsu, *Adv. Energy Mater.*, 2015, 5, 1501423.
- 35 J. K. Nørskov, T. Bligaard, J. Rossmeisl and C. H. Christensen, *Nat. Chem.*, 2009, **1**, 37–46.

- 36 D. Kim, J. Shi and Y. Liu, *J. Am. Chem. Soc.*, 2018, **140**, 9127–9131.
- 37 Q. Sun, Q. Wang, P. Jena and Y. Kawazoe, *J. Am. Chem. Soc.*, 2005, **127**, 14582–14583.
- 38 Y. Sun, A. Huang and Z. Wang, RSC Adv., 2019, 9, 26321-26326.
- 39 G. Feng, M. V. Ganduglia-Pirovano, C.-F. Huo and J. Sauer, *J. Phys. Chem. C*, 2018, **122**, 18445–18455.
- 40 A. Rasool, I. Anis, M. Dixit, A. Maibam, A. Hassan, S. Krishnamurty and M. A. Dar, *Catal. Sci. Technol.*, 2022, 12, 310–319.